

Local probing of charge and orbital-ordering-induced anisotropy with polarization-modulated infrared reflection difference microspectroscopy

J. S. Lee,^{1,*} M. Schmidt,² U. Schade,¹ S.-W. Cheong,³ and K. H. Kim^{4,†}

¹*Helmholtz-Zentrum Berlin für Materialien und Energie GmbH, Elektronen-Speicherring BESSY II, Albert-Einstein Strasse 15, Berlin 12489, Germany*

²*Department of Biomaterials, Max Planck Institute of Colloids and Interfaces, 14424 Potsdam, Germany*

³*Department of Physics and Astronomy, Rutgers University, Piscataway, New Jersey 08854, USA*

⁴*FPRD, School of Physics and Astronomy, Seoul National University, Seoul 151-747, South Korea*

(Received 18 November 2008; published 13 February 2009)

We investigated optical anisotropy of a $\text{Bi}_{0.3}\text{Ca}_{0.7}\text{MnO}_{3+\delta}$ crystal induced by charge and orbital orderings using infrared reflection difference microspectroscopy in combination with polarization modulation. Besides a drastic change in the anisotropic response below the charge ordering transition around 16 °C, we found an additional change in the optical anisotropy at a slightly lower temperature of around 13 °C, which is accompanied by a rotation of the optical axis by 45°. We attribute this intriguing behavior to the signature of the orbital ordering that is not coincident with the charge ordering transition with decrease in temperature.

DOI: 10.1103/PhysRevB.79.073102

PACS number(s): 78.20.-e, 78.30.-j, 71.30.+h

Anisotropic behavior is frequently observed in solid-state materials as a result of the spatial ordering of charge and spin degrees of freedom.¹ Typical examples are the one-dimensional stripe formation in the layered Cu and Ni oxides,^{2,3} and the cooperative ordering pattern of charge, spin, and orbital degrees of freedom in the Mn oxides.¹ Recently, Lee and co-workers^{4,5} demonstrated that layered manganese oxides can show in-plane anisotropy in the charge- and orbital-ordering (CO-OO) phase; the zigzag chain alignment of e_g orbitals in the MnO_2 plane gives rise to the electrical and optical anisotropies with respect to the direction of the orbital chain or stripe. As the orbital stripe rotates by 90° with a variation in temperature, the anisotropy axis was found to rotate accordingly.^{4,6} Such an intriguing anisotropy related with the orbital degrees of freedom was observed mainly in the layered manganese oxides. Therefore, it would be interesting to investigate such manifestation of the CO-OO state through the optical anisotropy in other manganese oxides having different crystal symmetries such as a simple perovskite.

In studying the optical anisotropy induced by orbital ordering, there are a few important technical issues to be pointed out. First, the orbital-driven anisotropy is expected to be much smaller than conventional anisotropy induced by the charge or spin degrees of freedom. Second, the twin-free single crystal is sometimes difficult to achieve and the typical domain size ranges from 10 to a few 100 μm at most. Third, the infrared wavelength region is of particular interest since many of the anisotropic properties appear in this spectral range.^{6,7} In these respects, polarization-modulated infrared reflection difference microspectroscopy, which was implemented recently,⁸ would be one of the most powerful tools to address these issues. It can resolve spectrally and spatially the anisotropy of solids in the midinfrared region. In particular, the modulation of light makes reference-free measurements possible, and thus enables to resolve small anisotropy with high sensitivity.

In this Brief Report, we exploited this technique to investigate the optical anisotropy of $\text{Bi}_{0.3}\text{Ca}_{0.7}\text{MnO}_{3+\delta}$ near the

CO-OO phase boundary. Across the charge ordering transition, we observed a drastic change in the anisotropic response. Furthermore, at a slightly lower temperature, we found an additional change in the anisotropic property, i.e., the rotation of the optical axis by 45°. We discuss this intriguing behavior based on the zigzag chain alignment of e_g orbitals forming an orthorhombic structural symmetry.

A $\text{Bi}_{0.3}\text{Ca}_{0.7}\text{MnO}_{3+\delta}$ sample was grown by the flux method,^{9,10} and it has a size of $\sim 2 \times 2 \times 2 \text{ mm}^3$. The optical experiments were carried out on the infrared microscope (Nicolet Continuum coupled to a Nexus 870 FT-IR spectrometer) of the infrared beamline IRIS at the electron storage ring BESSY II.¹¹ The confocal microscopic reflection measurements were performed at atmospheric pressure using synchrotron radiation, a 32 \times Cassegrain objective with a numerical aperture of 0.65, a rotatable sample mount, and a $\text{Hg}_{1-x}\text{Cd}_x\text{Te}$ detector. The temperature of the sample was controlled by Peltier elements. A dedicated apparatus for polarization modulation and its implementation in infrared reflection difference microspectroscopy are described in detail elsewhere.^{8,12,13} Importantly, the so-called photoelastic modulator (Hinds Instruments, PEM 90 II, ZnSe, 50 kHz) modulates the light beam between two perpendicular, linearly polarized states at a frequency of 100 kHz. Each measurement gives two acquired spectra simultaneously, i.e., the difference and the sum spectrum derived from the detected spectral intensities for each polarization state. Without measuring a reference, the ratio between the difference and the sum spectrum, here termed polarization modulation-reflection difference (PM-RD) spectrum, directly yields the normalized experimental reflection difference spectrum which is proportional to the anisotropy of the sample.

By using a visible microscope, we could distinguish several crystallographic domains in the whole sample area. In Fig. 1(a), we show a part of the sample containing mainly two distinct domains named A and B, which has an optical surface of the ac (or bc) and ab plane, respectively. Using a static polarizer we obtained the absolute reflectivity spectra along the optical axis of each domain at 18 °C in the normal

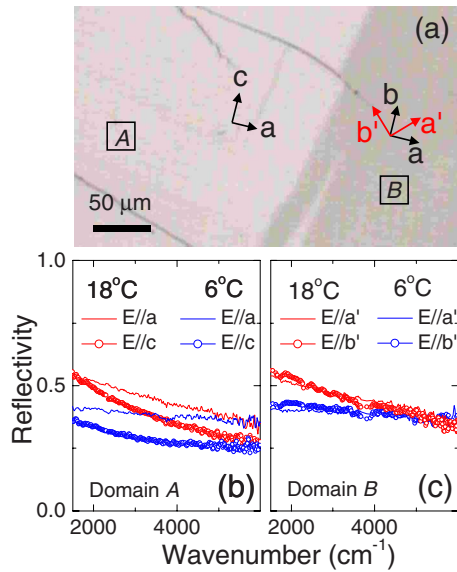


FIG. 1. (Color online) (a) Visible image of the $\text{Bi}_{0.3}\text{Ca}_{0.7}\text{MnO}_{3+\delta}$ crystal at 8°C . Two different domains showing contrast are marked with A and B. Absolute reflectivity spectra of the $\text{Bi}_{0.3}\text{Ca}_{0.7}\text{MnO}_{3+\delta}$ crystal along the optical axes of the domains (b) A and (c) B at two different temperatures of 18 and 6°C .

state and at 6°C in the CO state. For the domain A [see Fig. 1(b)], the spectra at 6°C along both directions show a smaller reflectivity than the respective ones at 18°C with a crossover around $6000\ \text{cm}^{-1}$. This behavior is attributable to the CO gap opening in this spectral region.⁷ While the optical response along each direction shows the same trend, the difference between the reflectivity spectra of each axis becomes larger at 6°C indicating a larger optical anisotropy in the CO state. In the case of the domain B, we found little polarization dependence of the reflectivity spectra. In Fig. 1(c), we displayed the spectra along the optical axes defined in the orthorhombic state, i.e., the a' and b' axes. The spectra along each axis overlap each other, and they show the smaller reflectivity in the CO state like in the domain A. Note that the spectra along both axes resemble the spectra along the a axis in the neighboring ac domain, as expected.

In order to examine the optical anisotropy of each domain in more detail, we adopted polarization-modulated midinfrared microspectroscopy. Figure 2 shows PM-RD spectra of

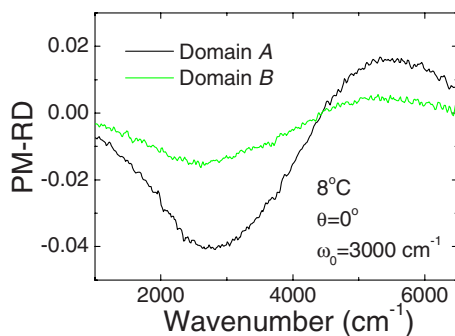


FIG. 2. (Color online) Midinfrared PM-RD spectra at 8°C for two different domains A and B as indicated in Fig. 1(a).

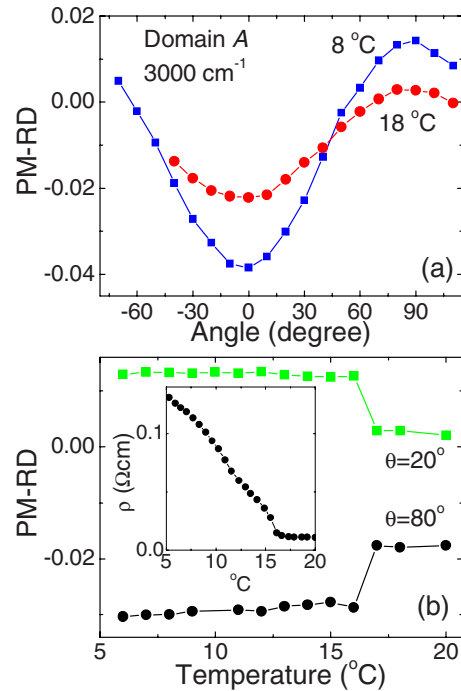


FIG. 3. (Color online) (a) Angular dependence of the PM-RD value for the domain A taken at 18 and 8°C . (b) Temperature dependence of the PM-RD value at sample rotation angles of 20° and 80° . All the values were taken from the PM-RD spectra at $3000\ \text{cm}^{-1}$. The inset displays a temperature-dependent dc-resistivity showing an abrupt increase with the charge ordering transition at $T_{\text{CO}} \sim 16^\circ\text{C}$.

the domain A and B at 8°C , each recorded for less than 1 min with a sampling spot size of $20 \times 20\ \mu\text{m}^2$. For the spectra shown here and afterward, the sample was rotated by θ with respect to the a axis of the domain A around the axis normal to the surface. The θ value is set to 0° for the spectra in Fig. 2. The spectral responses show sinusoidal behavior over the spectral range, having a maximum amplitude around $3000\ \text{cm}^{-1}$. This effect is due to the polarization modulation and, in particular, the wave-number-dependent modulator efficiency.¹⁴ Here, the modulator efficiency was optimal at $3000\ \text{cm}^{-1}$, where the $\lambda/2$ peak retardation was set. In the whole frequency range including $3000\ \text{cm}^{-1}$, the domain B has smaller PM-RD values than the domain A, which is consistent with the behaviors in the absolute reflectivity shown in Figs. 1(b) and 1(c). In the following we investigated the anisotropic properties of the domains A and B in detail as a function of the sample rotation angle and temperature.

Figure 3(a) shows the azimuthal angle (θ)-dependent PM-RD signal, corresponding to the spectral values at $3000\ \text{cm}^{-1}$, for the domain A recorded at 8°C and 18°C . While the angular dependences follow the same trend, the amplitude of the modulation at 8°C is about twice as large as the amplitude at 18°C . The finite anisotropy at 18°C should come from the crystallographic anisotropy between the a (or b) axis and the c axis as was observed in other perovskite manganites.^{7,15,16} As shown in Fig. 3(b), the PM-RD responses at the sample rotation angles of 20° and 80° exhibit abrupt changes around 16°C . Around the same

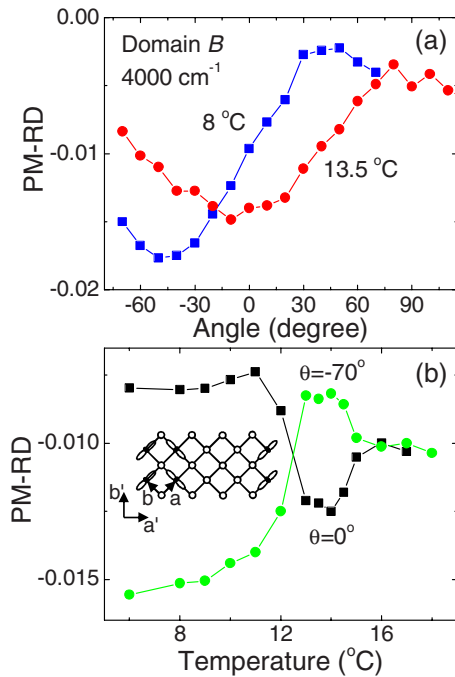


FIG. 4. (Color online) (a) Angular dependence of the PM-RD value for the domain *B* taken at 13.5 and 8 °C. (b) Temperature dependence of the PM-RD value at the sample rotation angles of 0° and -70°. All the values were taken from the PM-RD spectra at 4000 cm⁻¹. The inset of (b) shows a proposed charge-orbital ordering pattern for the Bi_{0.3}Ca_{0.7}MnO_{3+δ} crystal below 13 °C where Mn³⁺ (Mn⁴⁺) ions are specified by closed (open) circles with 3x²-r²/3y²-r² orbital.

temperature, we found an abrupt increase in the dc resistivity [inset of Fig. 3(b)], which is a typical signature of the CO transition in the Mn oxides.^{6,7} Therefore, the larger amplitude of the PM-RD below 16 °C can be attributed to the increase in the optical anisotropy with the charge ordering transition.¹⁷

Compared to the domain *A*, the domain *B* exhibits a rather complicated behavior in the optical anisotropy. To get a better signal we changed the PEM setting to have a $\lambda/2$ peak retardation at 4000 cm⁻¹. Figure 4(a) shows the angular dependence of the PM-RD signal at 8 and 13.5 °C. Above the CO transition temperature, e.g., at 18 °C, the PM-RD signal exhibits a very small amplitude (less than 10⁻³), and it is not easy to estimate the modulation phase. However, for the curves obtained at 13.5 and 8 °C, we clearly find that they have completely different phases while the PM-RD signals show comparable amplitudes; the PM-RD values at 13.5 and 8 °C have a maximum at about 0° and -45°, respectively. Note that the modulation at 13.5 °C has the same phase as the two curves of the domain *A* shown in Fig. 3(a).

Figure 4(b) shows the temperature dependence of the PM-RD signal at the sample rotation angles $\theta=0^\circ$ and -70° . There are three temperature ranges where the anisotropic responses exhibit distinct behaviors. First, at $T > 15$ °C, the values at $\theta=0^\circ$ and -70° are similar with each other. As was noted above, the anisotropic response is very small in this temperature range. Second, for $13 < T < 15$ °C, the PM-RD values exhibit a strong temperature dependence similar to the

behavior for the domain *A*. The values at $\theta=0^\circ$ (-70°) become larger (smaller) and a finite anisotropy could be observed as shown in Fig. 4(a). Third, at $T < 13$ °C the PM-RD values experience an additional change. The trend in the PM-RD values at 0° and -70° is opposite to those in the second temperature range. Note that the dc resistivity also shows a small but non-negligible change at the similar temperature [inset of Fig. 3(b)]. While the first change around 15 °C can be related to the CO transition like the change observed for the domain *A*, the second anomaly near 13 °C implies the existence of another phase transition accompanied by the rotation of the optical axis by 45°.

The anisotropic response and its temperature-dependent anomaly observed in the domain *B*, which has the *ab*-plane as the optical surface, is rather unexpected, and they remind us of the in-plane optical anisotropy recently reported in the layered manganites.^{4,6} It is interesting to note that while the optical axis in the layered manganites rotates by 90° as a function of temperature,⁶ the rotation of the optical axis in the Bi_{0.3}Ca_{0.7}MnO_{3+δ} sample occurs by 45°. Since the anisotropy in the conventional CO state of the manganese oxides is expected in the *ac* or *bc* plane and not within the *ab* plane,⁷ the possible origin of the *ab*-plane anisotropy can be attributed to the orbital degrees of freedom in cooperation with the charge ordering.

Before discussing the anomaly at 13 °C, let us look into the change in the anisotropic response just below 15 °C shown in Fig. 4(b). Considering the large anisotropy between the *a* axis (or *b* axis) and the *c* axis as shown in Fig. 3, it is natural to think about a finite contribution of the *c* axis in the optical surface of the domain *B* through the slight tilting of the sample. In this case, one can expect such contribution even in the normal state as in the *ac* plane of the domain *A* [see Fig. 3(a)], which is not the case for the present result. Actually, the multidomain nature of the crystal itself can drive an additional optical anisotropy in the *ab* plane in terms of the internal strain. Across the CO transition, while the lattice constant of the *c* axis decreases, those of the *a* and *b* axes increase.^{7,9,18} Such anisotropic lattice distortion can make the lattice constants of the *a* and *b* axes shorter or longer than the original ones owing to their interaction with the *c* axis of the neighboring domain. For instance, if the *b* axis in the *ab* domain and the *c* axis of the neighboring *ac* domain are lying parallel to the domain boundary, as shown in Fig. 1(a), the expansion of the *b* axis in the *ab* domain with the CO transition could be reduced since the *c* axis of the neighboring *ac* domain can induce internal strain by decreasing its lattice constant. In this case, the anisotropic axes in the *ab* domain should be defined in the same way as those of the *ac* domain as was actually observed in our experiment.

A further decrease in the temperature below 13 °C induced a rotation of the optical axis in the *ab* domain by 45°. We propose that this intriguing behavior can be understood by the CE-type charge and orbital ordering as depicted in the inset of Fig. 4(b). In this zigzag chain alignment of *e_g* orbitals, the transfer integral along the chain direction is larger than along the interchain direction which can lead to the optical anisotropy with respect to the direction of the orbital chain or stripe.⁴⁻⁶ Since this ordering accompanies the structural transition to the orthorhombic symmetry, the anisotropy

axes, i.e., a' and b' axes are defined differently from the cubic axes, i.e., a and b axes, rotated by 45° consistently with the experimental observation.

It should be noted that in the $\text{Bi}_{0.3}\text{Ca}_{0.7}\text{MnO}_{3+\delta}$ crystal studied here the orbital ordering transition does not occur simultaneously with the CO transition but at a slightly lower temperature. Here we suggest two possible candidates to explain this intriguing phenomenon. First, the internal strain coming from the multidomain, which we assumed as one of the origins of the finite anisotropy in the ab plane at $13 < T < 16^\circ\text{C}$, can delay the structural transition related with the OO. Second, as in the layered manganite the transition at 13°C can be one of two successive orbital-ordering transitions while the other one occurs at 16°C simultaneously with the CO transition. In this case, the anisotropic response in the ab plane can be coming from the ac or bc plane OO correlation coincident with the CO followed by the long-range ab plane OO correlation, as discussed above. In order to get a better understanding, more quantitative ap-

proach is necessary based on precise structural information.

In summary, we investigated anisotropic optical properties of $\text{Bi}_{0.3}\text{Ca}_{0.7}\text{MnO}_{3+\delta}$ in the charge- and orbital-ordered state by using polarization-modulated infrared reflection difference microspectroscopy. An abrupt development of the optical anisotropy was observed as the compound crossed over into the charge-ordered state. More interestingly, we found an additional change in the anisotropic response in the ab plane of the sample. Since it is accompanied by the rotation of the optical axes by 45° , we conclude that it originates from the orbital ordering in a zigzag chain accompanying the crystal symmetry change from the tetragonal to the orthorhombic structure.

Part of this work was supported by the Korean Research Foundation Grant and the Max Planck Society. K.H.K. is supported by NRL program (Grant No. M10600000238) by MOST, S. Korea. One of the authors (J.S.L.) acknowledges support from the Alexander von Humboldt Foundation.

*jslee@bessy.de

†optopia@snu.ac.kr

¹M. Imada, A. Fujimori, and Y. Tokura, *Rev. Mod. Phys.* **70**, 1039 (1998).

²J. M. Tranquada, B. J. Sternlieb, J. D. Axe, Y. Nakamura, and S. Uchida, *Nature (London)* **375**, 561 (1995).

³J. M. Tranquada, D. J. Buttrey, V. Sachan, and J. E. Lorenzo, *Phys. Rev. Lett.* **73**, 1003 (1994).

⁴Y. S. Lee, S. Onoda, T. Arima, Y. Tokunaga, J. P. He, Y. Kaneko, N. Nagaosa, and Y. Tokura, *Phys. Rev. Lett.* **97**, 077203 (2006).

⁵Y. S. Lee, Y. Tokunaga, T. Arima, and Y. Tokura, *Phys. Rev. B* **75**, 174406 (2007).

⁶Y. Tokunaga, T. Lottermoser, Y. Lee, R. Kumai, M. Uchida, T. Arima, and Y. Tokura, *Nature Mater.* **5**, 937 (2006).

⁷K. Tobe, T. Kimura, and Y. Tokura, *Phys. Rev. B* **69**, 014407 (2004).

⁸M. Schmidt, J. S. Lee, M. Grunze, K. H. Kim, and U. Schade, *Appl. Spectrosc.* **62**, 171 (2008).

⁹M. Rübhausen, S. Yoon, S. L. Cooper, K. H. Kim, and S.-W. Cheong, *Phys. Rev. B* **62**, R4782 (2000).

¹⁰S. Yoon, M. Rübhausen, S. L. Cooper, K. H. Kim, and S.-W. Cheong, *Phys. Rev. Lett.* **85**, 3297 (2000).

¹¹U. Schade, A. Röseler, E. H. Korte, F. Bartl, K. P. Hofmann, T. Noll, and W. B. Peatman, *Rev. Sci. Instrum.* **73**, 1568 (2002).

¹²M. Schmidt, U. Schade, and M. Grunze, *Infrared Phys. Technol.* **49**, 69 (2006).

¹³M. Schmidt, N. Gierlinger, U. Schade, T. Rogge, and M. Grunze, *Biopolymers* **83**, 546 (2006).

¹⁴L. A. Nafie and M. Diem, *Appl. Spectrosc.* **33**, 130 (1979).

¹⁵The average base line of the PM-RD values is not at the zero level but is found to have a negative value. This comes from, for example, polarization artifacts of the PEM and the optical setup. The amplitude of the PM-RD signal, however, is hardly affected by such artifacts (Ref. 8 and M. Schmidt *et al.*, to be published), hence it is a suitable indicator of the sample anisotropy irrespective of the experimental artifacts.

¹⁶Y. Tokura, *Rep. Prog. Phys.* **69**, 797 (2006).

¹⁷The angle-dependent PM-RD values can be fitted by a well-defined formula, as shown in Ref. 8, where the parameters used for the fitting were found to be consistent with the reflectivities shown in Figs. 1(b) and 1(c), with the reflectivity difference of, e.g., $\sim 10\%$ at 8°C for the domain A.

¹⁸W. Bao, J. D. Axe, C. H. Chen, and S.-W. Cheong, *Phys. Rev. Lett.* **78**, 543 (1997).